Thermochimica Acta, 16 (1976) 1–16

EFFECT OF ELECTRIC FIELDS ON THE DEHYDROXYLATION KINETICS OF PSEUDOBOEHMITE

K. J. D. MACKENZIE
Chemistry Division, D.S.I.R., Private bag, Gracefield, Wellington (New Zealand)
(Received 10 November 1975)

ABSTRACT

The dehydroxylation kinetics of pseudoboehmite were studied both in the presence and absence of an electric field using an electrolysis cell in conjunction with an X-ray furnace. At higher field strengths, the onset temperature of the reaction is lowered and the decomposition rate significantly increased by the electric field, particularly at the negative electrode, in which region the crystallite size is also greater. The activation energy for the reaction is not significantly changed by electrolysis.

The electrolysis mechanism is discussed in terms of cleavage of hydrogen bonds and the migration of the resulting protons to the cathode where they may be discharged as water or hydrogen, or may enter and stabilize the structure of the decomposition product.

INTRODUCTION

Pseudoboehmite, sometimes called gelatinous boehmite, is a hydrated aluminium oxide related to boehmite, γ-AlOOH, but containing 1.3–1.8 moles of excess water per mole Al_2O_3[1]. The excess water is believed[1] to be hydrogen-bonded between layers having boehmite structure; the stacking of these layers is imperfect, leading to a broad, diffuse X-ray diffraction pattern with spacings corresponding to the most intense lines of well-crystallized boehmite. Pseudoboehmite dehydrates at 300°C, forming a poorly crystalline phase described as either η- or γ-alumina[1] (both of these aluminas have a defect spinel structure, but differ in the type of disorder or degree of tetragonal distortion present)[1]. Well-crystallized boehmite also decomposes to form γ-alumina, but at higher temperatures than pseudoboehmite (450°C)[1].

Pseudoboehmite appears to play a practical role in the anodization of aluminium; it has been reported that this process occurs more rapidly and with increased current efficiency in the presence of a surface layer of pseudoboehmite[2], which is thought to contribute to the formation of the anodic oxide barrier by its decomposition to γ-alumina[2]. Although this reaction normally occurs at 300°C, Alwitt[2] has suggested that the decomposition temperature might be sufficiently lowered by the influence of the strong electric fields applied during anodization for

the reaction to occur at anodizing temperatures (commonly 90°C). The only previous study of the effect of electric fields on the decomposition of hydrous aluminium oxides was made on gibbsite, $Al(OH)_3$, and the results suggested[3] that the onset temperature for dehydroxylation of this material is not particularly sensitive to electric fields. The structure and composition of gibbsite is, however, rather different from that of pseudoboehmite, and, moreover, the electric field strengths used in the gibbsite experiments were much lower than those applied during anodization.

The present work was therefore undertaken on pseudoboehmite at higher field strengths in an attempt to provide further information on the role of pseudoboehmite in the aluminium anodizing process.

The progress of the decomposition was followed by X-ray diffractometry, using an X-ray furnace and electrolysis cell which allowed the samples to be monitored throughout the course of their electrolysis. The effect of the applied field strength on the reaction rate at both the negative and positive electrode faces was determined, and the decomposition kinetics at the anode and cathode were determined at the highest field strength (2.35×10^6 V m^{-1}). For comparison, the decomposition kinetics were also determined in the absence of the field. The effect of fields on the crystallite size and morphology of the γ-alumina product was studied by X-ray line broadening measurements and scanning electron microscopy (S.E.M.).

EXPERIMENTAL

The pseudoboehmite was prepared from amorphous $Al(OH)_3$ by a method published elsewhere[4]. The reaction time of amorphous hydroxide in boiling water was 5 min and the product was dried at ~40°C overnight, followed by heating at 85°C and ambient pressure for 9 h. The X-ray trace of the resulting white powder consisted of characteristically broad bands corresponding to the major pseudoboehmite lattice spacings reported by Papee et al.[5] and Alevra et al.[6]; the present spacings were slightly closer to those of Papee et al.[5]. No other crystalline phases were detected by X-ray diffraction. The i.r. spectrum of the present material was identical to that of the pseudoboehmite studied in ref. 4. The average weight-loss on ignition to 1160°C, determined in a Mettler Model 21 thermal analyser at heating rates of 6 and 10°C min^{-1} in ambient atmosphere, was 32.6%, representing 2.75 moles H_2O per mole anhydrous Al_2O_3. Since crystalline boehmite contains 1 mole H_2O per mole Al_2O_3, the excess water content of the present sample is 1.75 moles per mole Al_2O_3. The TG and DTG curves are shown in Fig. 1.

The electrolyses were carried out in a cell described elsewhere[7], and used in conjunction with a Stone XR-6 X-ray furnace, using Cu$K\alpha$ radiation. All firings were made in a dynamic atmosphere of dry, oxygen-free nitrogen (flow rate 2.5 ml sec^{-1}). The course of the reaction was followed by monitoring the disappearance of the 150 pseudoboehmite peak at $d = 1.854$ Å. This peak was chosen because unlike several other major peaks, it does not closely coincide with any major spacing of the γ-alumina product; it does, however, occur in the vicinity of a γ-alumina peak at

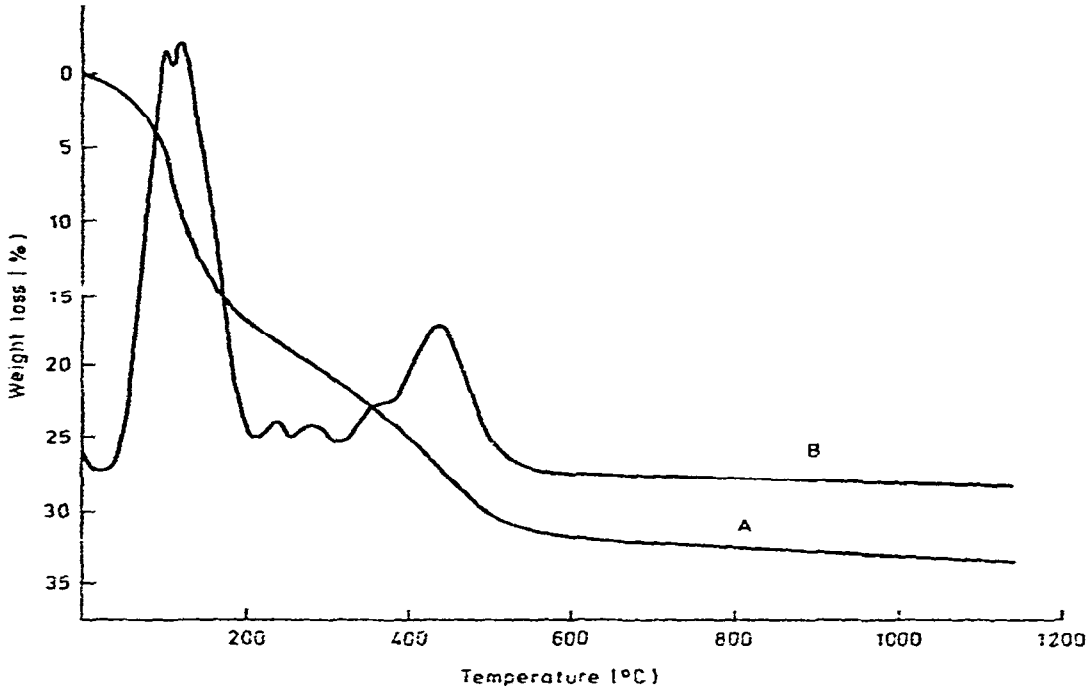

Fig. 1. Thermogravimetric curves for pseudoboehmite. Heating rate, 6 °C min^{-1}, in ambient atmosphere. (A) = TG curve; (B) = DTG curve.

$d = 1.96$–1.99 Å, allowing this to be also monitored during the reaction. The disappearance of the reactant was monitored in preference to the appearance of the product, because of the extremely poor crystallinity of the latter at the low reaction temperatures studied. The presence of a sharp platinum peak at 1.96 Å (from the platinum mesh upper electrode) did not interfere seriously with the γ-alumina peak because of the broadness of the latter; moreover, no quantitative measurements were made of the γ-alumina peak.

The degree of reaction was determined from the height of the pseudoboehmite peak rather than its area, because over the narrow temperature range of the reaction the shape of this peak was found to be constant. The reproducibility of the analysis technique was about 7%, similar to other quantitative X-ray powder methods.

After setting up and aligning the sample and measuring the room-temperature height of its 150 peak, the furnace was quickly brought to the desired reaction temperature, and the electrolysis voltage applied from a Philips PW4022 E.H.T. power supply. The goniometer was set to oscillate over the region of interest, the elapsed electrolysis time being measured from peak-to-peak on the recorder trace. Experiments were carried out both with the positive and negative electrode face in the X-ray beam.

To investigate the effect of electrolysis on the crystallite size and morphology of the γ-alumina product, some experiments were performed at 450 °C, at which

temperature the product was more crystalline. Crystallite size estimates were made from line-broadening measurements of the 400 γ-alumina peak[8], using a value of 0.9 for the shape factor k and applying the Warren correction for instrumental broadening[8], determined from measurements on well-crystallized γ-alumina prepared by calcining pseudoboehmite for several hours at 800 °C.

After reaction, samples of the upper electrode material were taken, mounted on aluminium stubs with double-sided cellulose tape, coated with a vacuum-deposited gold-palladium film and examined by scanning electron microscopy (S.E.M.).

RESULTS AND DISCUSSION

Kinetics of pseudoboehmite decomposition in the absence of a field

The kinetic curves for the decomposition of unelectrolysed pseudoboehmite are shown in Fig. 2.

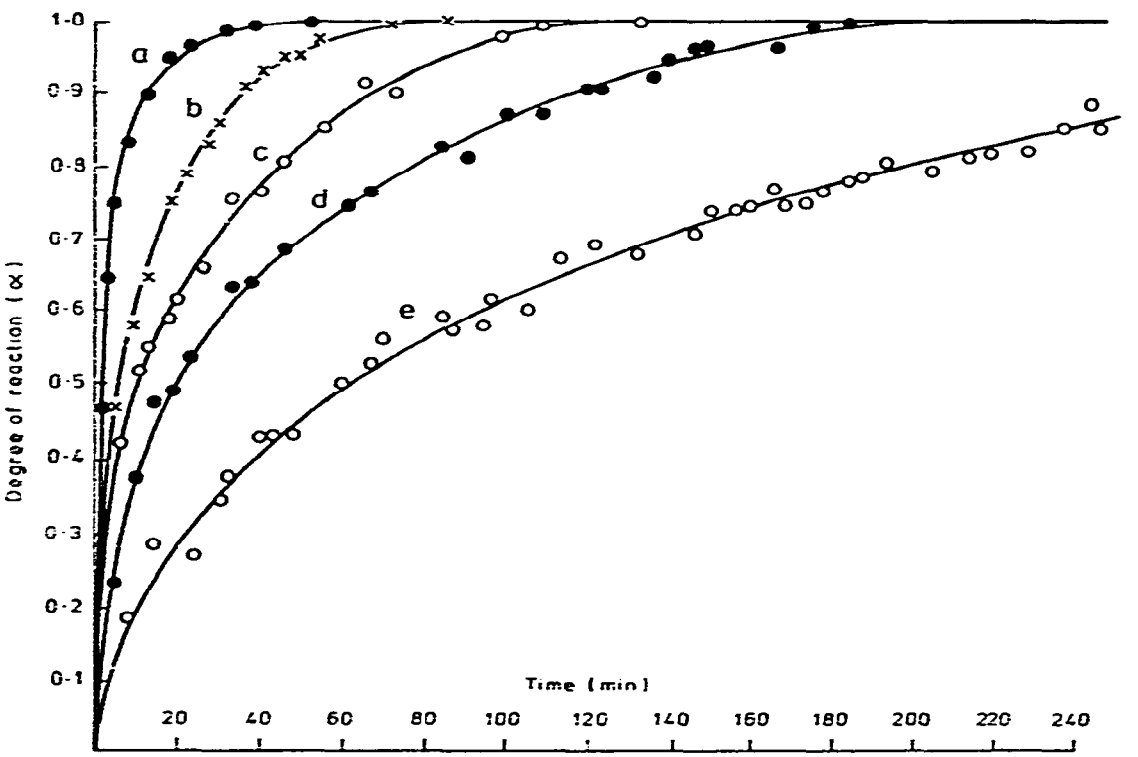

Fig. 2. Kinetic curves for dehydroxylation of unelectrolysed pseudoboehmite. (a) = 350 °C; (b) = 325 °C; (c) = 300 °C; (d) = 280 °C; (e) = 260 °C.

Attempts were made to fit these curves to several commonly used solid state reaction equations[9]. The data are fitted best by Jander's equation for diffusion-controlled reaction in a sphere, which has the form

$$(k/r^2)t = [1-(1-\alpha)^{1/3}]^2 = D(\alpha) \qquad (1)$$

where α is the fraction reacted in time t in a spherical particle of radius r, and k is the rate constant.

Other diffusion-controlled equations give theoretical curves of similar shape, and fit the data almost as well as eqn. (1). However, the data cannot be fitted to equations based on order-of-reaction, phase boundary control or nucleation and crystal growth. Although the rate-determining mechanism is fairly clearly diffusion-controlled, a distinction cannot properly be made on the basis of the present data, between the various equations arising from different types of diffusion processes.

The kinetic curves of the present experiments differ considerably from the curve shapes obtained in kinetic studies of the decomposition of crystalline boehmite[10,11] and diaspore[12] (α-AlOOH). The kinetic curves for these materials are characterized by long, flat initial portions showing no signs of parabolic behaviour and allowing a very simple kinetic analysis. The main difference between these crystalline materials and pseudoboehmite is the excess water in the latter. Although weight-loss curves published by Alevra et al.[13] show no clear distinction between structural and excess water, TG and particularly DTG curves determined at a slower heating rate on the present sample show at least two distinct but overlapping regions of water loss (Fig. 1). It seems reasonable that the rate of loss of the less tightly-bound water located in the interlamellar spaces of the structure should be controlled by diffusion of water from the system, and since this diffusion process overlaps with the loss of structural water from the boehmite-like regions, it would be expected to mask

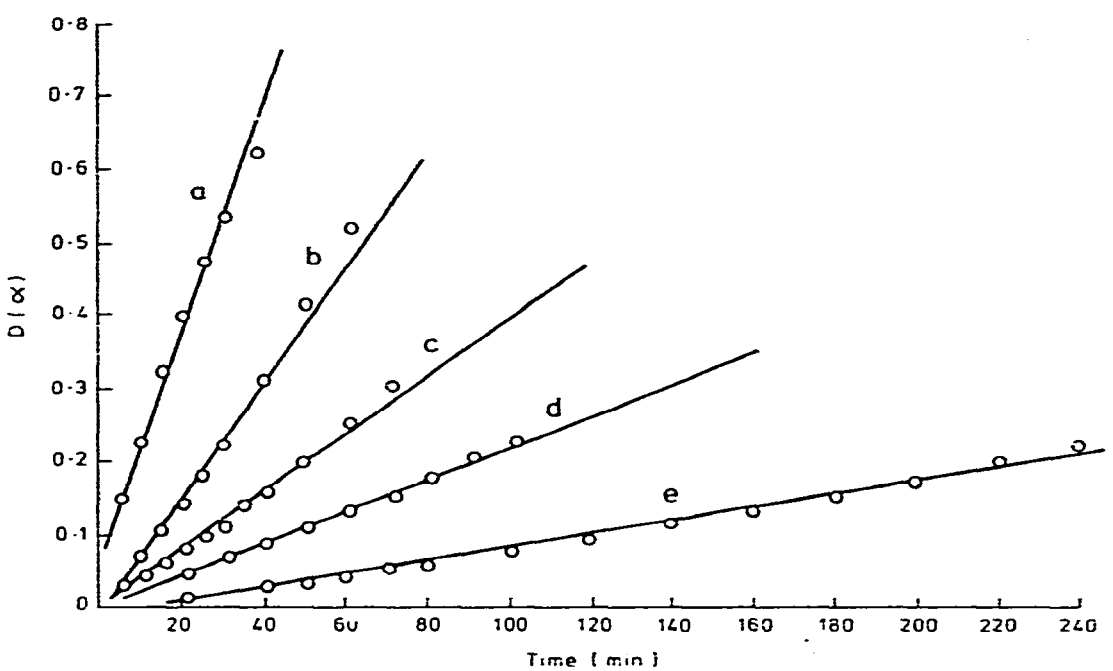

Fig. 3. Plots of D(α) (from Jander's equation) vs. time for unelectrolysed pseudoboehmite. (a) = 350 °C; (b) = 325 °C; (c) = 300 °C; (d) = 280 °C; (e) = 260 °C.

the initial kinetics of that process and lead to a quite different overall kinetic curve shape.

Rate constants for the reaction were obtained from the slopes of the least-squares straight lines fitted to plots of $D(\alpha)$ vs. t (Fig. 3), where $D(\alpha)$ is as defined in eqn. (1). The Arrhenius plot constructed from these rate constants is shown in Fig. 4, from which the apparent activation energy for the decomposition process is found to be 81 kJ mol^{-1}, with a pre-exponential factor A of 1.6×10^3 sec^{-1}.

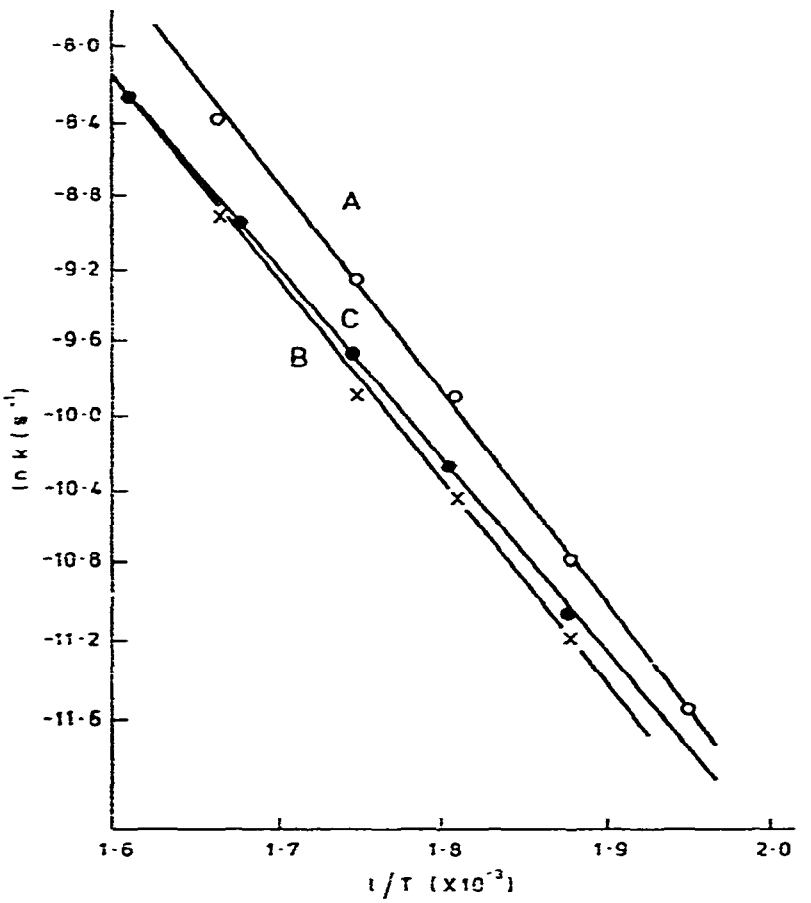

Fig. 4. Arrhenius plots for electrolysed and unelectrolysed pseudobochmite. Electrolysing field strength 2.35×10^6V m^{-1}. (A) = Electrolysed sample, negative face; (B) = electrolysed sample, positive face; (C) = unelectrolysed sample.

The kinetic analysis was completed by computing the activation free energy ΔG^* from

$$\Delta G^* = RT[\ln (RT/Nh) - \ln k] \quad (2)$$

where N is Avogadro's number and h is Planck's constant. The activation entropies

ΔS^* follow from

$$\Delta S^* = (E_a - \Delta G^*)/T \tag{3}$$

Values of the activation thermodynamic functions thus calculated are collected in Table 1.

TABLE 1

KINETIC PARAMETERS FOR ELECTROLYSED AND UNELECTROLYSED PSEUDOBOEHMITE IN FLOWING NITROGEN

Flow-rate = 2.5 ml sec^{-1}; electrolysing field strength = 2.35×10^6 V m^{-1}; current = 1.9 mA.

Sample	*T* (°C)	*k* ($\times 10^{-5}$ sec^{-1})	E_a ($kJ\ mol^{-1}$) ±10	*A* (sec^{-1})	ΔG^* ($kJ\ mol^{-1}$) ±7	ΔS^* ($J\ K^{-1}$) ±20
Unelectrolysed	350	25.0	81	1.6×10^3	199	−189
	325	12.9	81	1.6×10^3	194	−189
	300	6.52	81	1.6×10^3	189	−188
	280	3.63	81	1.6×10^3	185	−188
	260	1.53	81	1.6×10^3	182	−189
Electrolysed negative face	325	22.5	94	4.0×10^{-4}	192	−164
	300	9.33	94	4.0×10^{-4}	188	−164
	280	5.0	94	4.0×10^{-4}	184	−163
	260	2.08	94	4.0×10^{-4}	181	−163
	240	0.94	94	4.0×10^{-4}	177	−162
Electrolysed positive face	325	13.6	89	8.3×10^3	194	−176
	300	5.1	89	8.3×10^3	191	−178
	280	2.92	89	8.3×10^3	186	−175
	260	1.39	89	8.3×10^3	183	−176

Decomposition kinetics in the presence of a field

Kinetic experiments were performed using a field strength of 2.35×10^6 V m^{-1}, monitoring the anode kinetics in one set of experiments and the cathode kinetics in another set. The decomposition curves for the negative and positive faces are shown in Figs. 5 and 6, respectively. Equation (1) was found to fit both sets of curves satisfactorily, and the rate constants are given in Table 1. The corresponding Arrhenius plots are shown in Fig. 4, from which the activation energies for the negative and positive faces are 94 and 89 kJ mol^{-1}, respectively. The free energies and entropies of activation, calculated from eqns (2) and (3), are presented in Table 1.

Table 1 shows that throughout the temperature range of this study, the decomposition rates at the negative electrode face are considerably increased by electrolysis, whereas the rates at the positive face are not much different from those of the unelectrolysed samples. By increasing the reaction rate at the cathode, electrolysis effectively lowers the temperature at which the reaction in that region becomes kinetically significant, i.e., the apparent onset temperature is lowered. The

effect of the field in these studies is a kinetic effect only: the reaction rate data give no direct information about the effect of electric fields on the thermodynamic stability of the reactant, and product phases which may also be influenced by the electric field.

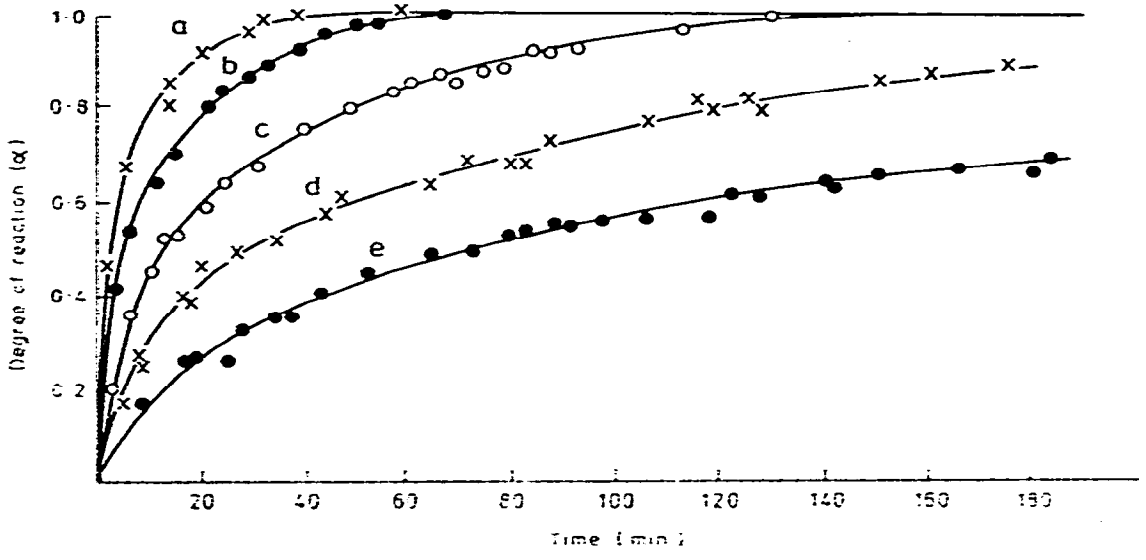

Fig. 5. Kinetic curves for dehydroxylation of electrolysed pseudoboehmite, negative face. field strength 2.35×10^6V m^{-1}. (a) = 325 °C; (b) = 300 °C; (c) = 280 °C; (d) = 260 °C; (e) = 240 °C.

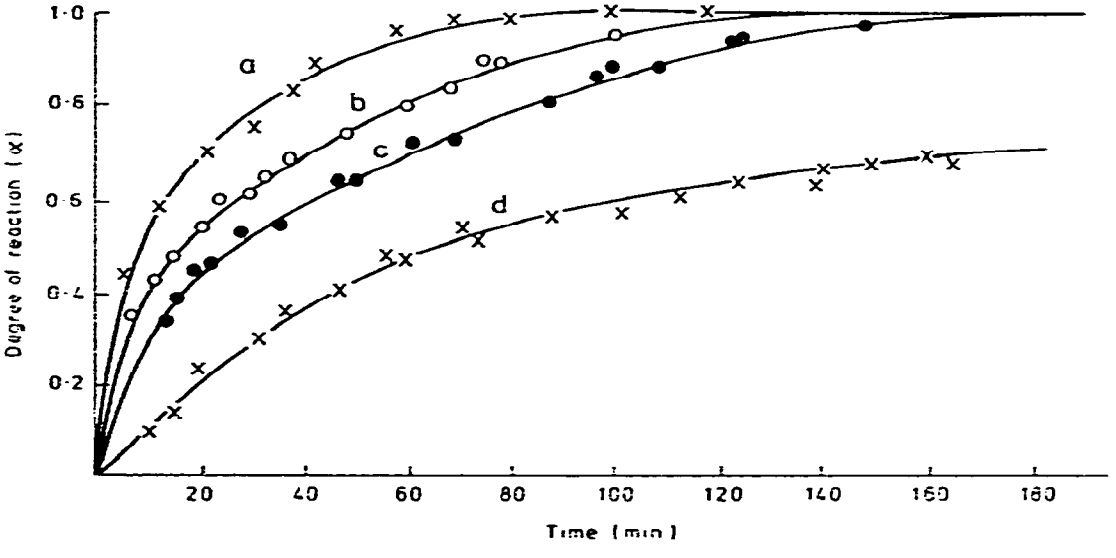

Fig. 6. Kinetic curves for dehydroxylation of electrolysed pseudoboehmite, positive face. field strength 2.35×10^6V m^{-1}. (a) = 325 °C; (b) = 300 °C; (c) = 280 °C; (d) = 260 °C.

The activation energies reported here are only slightly different in the electrolysed and unelectrolysed samples, but although within the estimated experimental uncertainty, the slight increase in activation energy of the electrolysed samples may reflect a small but real tendency for the temperature range over which the reaction proceeds to be narrowed by the field. Activation energies for pseudoboehmite decomposition have not previously been reported, but the present values may be compared with those of the crystalline monohydrates diaspore and boehmite. The two reported values for boehmite (176 kJ mol^{-1} in vacuum[10] and 293 kJ mol^{-1} in nitrogen[11]) are both much higher than the present energies, which are, however, very similar to the activation energy for diaspore (101 kJ mol^{-1})[12]. The similarity between E_a for diaspore and the diffusion energy of protons through a hydrous oxide lattice (69 kJ mol^{-1}) has been cited[12] as evidence for a diffusion-controlled mechanism in diaspore and its analogue goethite. A similar argument might well be applied to pseudoboehmite, and is consistent with the fitting of the kinetic curves by a diffusion equation.

The negative sign of the activation entropies indicates that the transition state for the reaction is more ordered than the reactant. The slightly less negative ΔS^*values of the electrolysed samples suggest that ordering is not assisted by the field, possibly due to the more rapid decomposition of the electrolysed samples, particularly at the negative electrode.

Effect of field strength on the dehydroxylation rate

The rate constants derived from kinetic experiments at 325°C are shown in Fig. 7 as a function of the applied field strength. At lower fields the dehydroxylation rate at both the negative and positive electrode faces is decreased relative to the unelectrolysed sample, but at higher field strengths the rates are increased by the field, particularly at the negative electrode. Although the behaviour at the negative electrode suggests that the rate should continue to increase at still higher field strengths (i.e., fields such as encountered under anodizing conditions), predictions made by extrapolating Fig. 7 to much higher fields should be treated with caution, since the electrolysis behaviour could alter markedly at anodizing fields, due to space charge effects and saturation polarization. However, the 40% increase in reaction rate at the negative electrode under the highest field strengths investigated here should be at least equalled and probably bettered at even higher field strengths.

Effect of electrolysis on particle size and morphology

The results of the S.E.M. and X-ray particle size measurements on samples reacted at 450°C are shown in Table 2, from which it is seen that the fundamental crystallite size at the cathode is almost double that of the anode material, the size of which is only slightly larger than in the unelectrolysed samples. This trend is not reflected in the gross morphology of the crystallite clusters, as shown by S.E.M. Moreover, the S.E.M. photographs showed that the appearance of both the electrolysed and unelectrolysed samples was similar to the undecomposed material. The

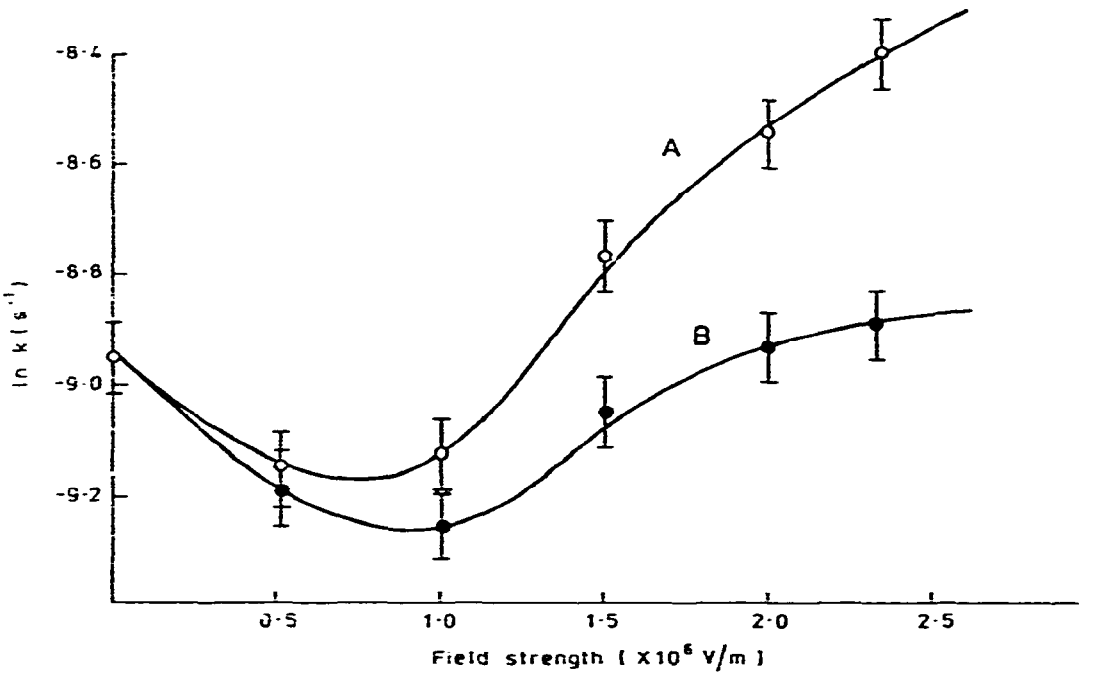

Fig. 7. Variation of rate constant for electrolysed pseudoboehmite with applied field strength a 325°C. (A) = Negative face; (B) = positive face.

TABLE 2

PARTICLE SIZE DETERMINATIONS OF γ-ALUMINA FROM ELECTROLYSED AND UNELECTROLYSED PSEUDOBOEHMITE REACTED AT 450°C

	Sample		
	Unelectrolysed	*Negative face*	*Positive face*
X-ray crystallite size (Å)[a]	27	50	35
S.E.M. particle size (μm)[b]	9.7	12.0	14.4

[a] Estimated from mean of experimental points recorded during 90–140 min of elapsed reaction time. Standard error = ±3.5 Å. [b] Estimated from S.E.M. micrographs of samples reacted for 140 min. Standard error = ±2.5 μm.

appearance of the γ-alumina product was not much more crystalline even after, calcining at 600°C, emphasising the disordered nature of the decomposition product of pseudoboehmite.

Effect of electrolysis on the reaction mechanism

The dehydration mechanism in unelectrolysed boehmite involves the removal of several types of water, namely mechanically-held (loosely-bound) water, inter-

lamellar hydrogen-bonded water, and structural hydroxyl water. Although the binding strength of each type of water is expected to be different, leading to differences in the temperature and activation energy of evolution for each type, in practice there is considerable overlap, and water evolution occurs over a wide temperature range (Fig. 1, curve A). The kinetics reported here were based on the disappearance of an X-ray spacing associated with the boehmite structure and should therefore pertain to the removal of structural hydroxyl water; this process and its kinetics is, however, unlikely to be totally independent of the concomitant dehydration processes. Moreover, the destruction of the boehmite lattice by dehydroxylation cannot be taken to indicate the complete loss of water since the γ-alumina product is stabilised by protons, being able to accommodate up to 0.2 moles of water per mole Al_2O_3[14]. The TG curves (Fig. 1) indicate that at 600°C, 0.25 moles H_2O are still present, while at 900°C (the temperature at which γ-alumina from pseudoboehmite transforms to δ-alumina)[1], the structure still contains about 0.02 moles H_2O per mole Al_2O_3. Thus, the γ-alumina which recrystallizes after dehydroxylation contains about 0.05 moles of water in excess of the maximum amount tolerated by the fully protonated spinel HAl_5O_8. The excess water is thought[14] to reside on the surface of the oxide as hydroxyl groups bound to the surface oxygen atoms.

The dehydration mechanism in unelectrolysed pseudoboehmite begins with the thermal cleavage of the interlamellar hydrogen bonds, with the release of water which diffuses from the system. At higher temperatures, dehydroxylation sets in, probably by a mechanism similar to that in crystalline boehmite, which has been studied by i.r. spectroscopy[15], electric conductance and diffusion measurements[16] and proton magnetic resonance[17]. These studies suggest that immediately prior to dehydroxylation, the protons in the structure reversibly assume a "predehydroxylation state"[15], in which they either move to a neighboring but less stable position, "flip" between two equilibrium positions in the neighborhood of some particular oxygen atom, or are delocalized over all the oxygens in the system. At the dehydroxylation temperature, boehmite contains a high concentration ($\sim$10%) of protons associated with lattice defects of the type $^+OH_2$ or O^- which arise from the capture of one proton of the boehmite chain by an adjacent hydroxyl[17]:

$$Al\text{–}OH + OH\text{–}Al \rightarrow Al\text{–}{}^+OH_2 + Al\text{–}O^- \qquad (4)$$

The strong repulsion between $^+OH_2$ units assists diffusion of water out of the lattice[17]. The postulated occurrence of $^+OH_2$ and O^- defects in microregions of the boehmite crystallites[17] suggests that dehydroxylation might take place by an inhomogeneous mechanism[18] involving migration of protons to "donor regions" from which water is ultimately lost, and a counter-migration of Al^{3+} to "acceptor regions" which ultimately become γ-alumina. The process is shown schematically in Fig. 8, in which the γ-alumina phase is shown fully protonated, in accordance with the TG data. The transformation of boehmite to γ-alumina involves virtually no disruption of the oxygen structure, which remains essentially cubic close packed throughout[1], supporting an inhomogeneous rather than a homogeneous mechanism; the latter

would involve considerable disruption of the oxygen structure. Similar considerations have led to the suggestion of an inhomogeneous dehydroxylation mechanism for diaspore[12].

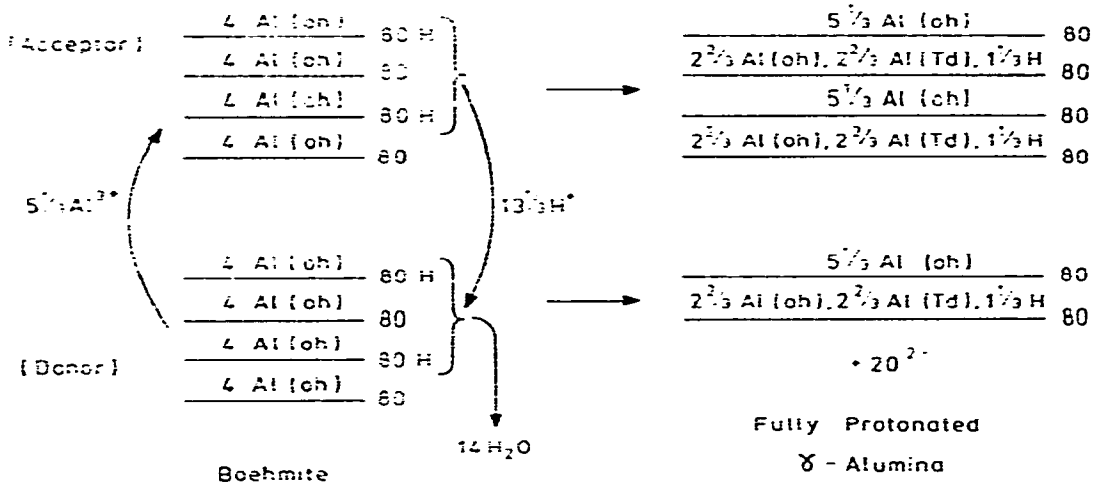

Fig. 8. Schematic representation of the proposed inhomogeneous mechanism for dehydroxylation of unelectrolysed pseudoboehmite.

In considering the possible effect of electric fields on this reaction, account must be taken of the various ionic movements involved. These may be summarised as:

(a) Loss of interlamellar water by rupture of hydrogen bonds.

(b) Migration of protons to extrinsic defect sites, forming $^{+}OH_2$ species which are removed from the lattice by diffusion.

(c) Change in coordination of Al from distorted octahedral sites in boehmite to a spinel structure containing both octahedral and tetrahedral aluminium ions, and with cation vacancies randomly distributed over the tetrahedral positions[19].

(d) Stabilization of the tetrahedral vacancies by protons.

Since the product of step (a) is molecular water, it would not be expected to be influenced much by external fields, apart from a possible change in hydrogen bond strength due to polarization in the field. In this connection it is interesting to compare the strength of the hydrogen bond in pseudoboehmite with the increase in total polarization energy induced in the sample by the field. An order of magnitude estimate of the latter is obtained by considering the material as a dielectric, in which the increase in energy per unit volume due to an electric field is given[20] by

$$dF = \varepsilon_s(E^2/8\pi) \tag{5}$$

where ε_s is the static dielectric constant and E is the field strength. Following Mata Arjona and Fripiat[16], the static dielectric constant is taken to be of similar magnitude to the optical dielectric constant ε_∞, which can be further approximated to the square of the mean refractive index, if the small contribution from the elastic displace-

ment of the dipoles is ignored. At typical field strengths of the present experiments ($\sim 2 \times 10^6$ V m^{-1}), the energy increase in the dielectric is of the order of 6×10^{11} J m^{-3}, or about 100 kJ within the sample volume of the present experiments (1.68×10^{-7} m^3). Since this sample volume contains about 1.7×10^{21} hydrogen bonds, the energy increase due to the field is about 6×10^{-17} J per bond. This energy is comparable with the average bond strength of a hydrogen bond (about 25 kJ mol^{-1}, or about 4×10^{-20} J per bond)[21], and on this reasoning, it seems likely, that at least those hydrogen bonds lying in the axis of the applied field could be weakened by the field to the point of rupture before sufficient thermal energy had been supplied to thermally cleave these bonds. This effect would not be confined to any particular electrode region but should occur throughout the volume, provided the field was homogeneous within the sample.

Steps (b) and (d) involve proton movements, which are likely to be significantly influenced by the field, particularly when in the delocalized state immediately preceding dehydroxylation. Electrical conductance measurements on boehmite[16] suggest that protons migrate by the formation of a proton vacancy with the simultaneous displacement of this proton towards an interstitial position. The energy involved in proton vacancy formation ($\sim$46 kJ mol^{-1}) is of a similar magnitude to the energy level of the potential barrier at which the tunnelling probability per period of stretching vibration approaches unity[16], while the activation energy for interstitial proton displacement is 21.3 kJ mol^{-1} (ref. 16).

The stabilization energy of γ-alumina spinel by protons as in step (d) is very difficult to estimate, but an indication of its magnitude can be gained from the stabilization energy of the isomorphous lithium-spinel $LiAl_5O_8$. The stabilization energy due to the presence of the lithium in the spinel is reflected in the difference between the formation enthalpies of the lithium compound and a comparable unit of γ-alumina. The heat-of-formation of $LiAl_5O_8$ at 957 K has been reported[22] as 131.25 kJ mol^{-1}, from which the heat-of-formation from the elements is -4398.2 kJ mol^{-1}. A reliable estimate of the formation enthalpy of γ-alumina is not easy to obtain, but after surveying the available data, Kusov[23] adopted a value of -1660.3 kJ mol^{-1} Al_2O_3 at 978 K, giving a value of -4151 kJ for the comparable unit $Al_5O_{7.5}$. Thus, the presence of lithium in this spinel increases its stability by 247.5 kJ (or 99.1 kJ, referred to one mole of Al_2O_3). This stabilization energy value cannot be applied to the fully protonated alumina spinel directly, because of the difference in size between Li^+ and H^+. In general, however, tetrahedral ions of smaller size form more stable spinels; this is confirmed by using the data of Navrotsky and Kleppa[24] to calculate standard formation enthalpies of the aluminates of Mg^{2+}, Zn^{2+}, Co^{2+} and Fe^{2+}, all of which are essentially normal spinels with the divalent ions in tetrahedral sites. The standard formation enthalpies become increasingly negative with decreasing radius of the tetrahedral ion, and on this basis it seems reasonable that the stabilization energy of HAl_5O_8 should be at least as great as that estimated for $LiAl_5O_8$, and possibly considerably greater.

The energy involved in step (c) is the octahedral site preference energy of Al^{3+},

estimated by Navrotsky and Kleppa[25] to be -44.3 kJ mol^{-1} for a structure containing vacancies on tetrahedral sites, as is probably the case with dehydroxylated pseudoboehmite[19].

The effect of electrolysis on the rate of the dehydroxylation reaction can therefore be explained in terms of several field-dependent steps. In the first instance, the field assists the rupture of appropriately aligned hydrogen bonds throughout the reactant volume, thus lowering the onset temperature of the reaction. Protons resulting from the dissociation of this water then migrate towards the cathode by a low activation energy interstitial mechanism, leading to an increase in the $^{+}OH_2$ concentration at the cathode and increased vacancy concentrations at the anode. In terms of the inhomogeneous mechanism, the cathode may be envisaged as the donor region and the anode as the acceptor region. It is unlikely that the aluminium ions will migrate counter to the electric field direction as might be inferred by analogy with the inhomogeneous mechanism proposed for unelectrolysed pseudoboehmite; under electrolysis the aluminium ions probably undergo virtually no migration because of their relatively low electric mobility. During the course of the reaction, however, some of the aluminium ions change their co-ordination number; this is a consequence of the crystal changes due to structural water loss, and should be influenced by the electric field only insofar as dehydroxylation is field-dependent.

Two reactions may then occur at the cathode:

$$^{+}OH_2 + e^{-} \rightarrow H_2O \tag{6}$$

$$2H^{+} + 2e^{-} \rightarrow H_2 \tag{7}$$

Both reactions (6) and (7) involve the removal of protons from this region. The evolution of hydrogen from hydrous aluminium oxide by a redox reaction during dehydroxylation has been previously reported[26]. In addition, a further reaction can be envisaged in the cathode region, by virtue of the high concentration of protons present there:

$$\square_{\frac{1}{3}}Al_{5\frac{1}{3}}O_8 + H^{+} \rightarrow HAl_5O_8 + \tfrac{1}{3}Al^{3+} \tag{8}$$

Reaction (8) should also enhance the decomposition, since it leads to the formation of a product with an increased stabilization energy. Thus, dehydroxylation would be expected to proceed faster in the cathode region than at the anode, since the elements of water are removed from the former by the electrolysis process as well as by the normal thermal diffusion processes. A high concentration of water at the cathode, both in the solid and in the atmosphere immediately adjacent, should give rise to larger crystallite sizes, since crystallite growth in oxides is enhanced under humid conditions[7]. The stabilization of the decomposition product by protons also suggests that the formation temperature of this phase might be lowered by electrolysis, i.e., electrolysis should assist both the low-temperature decomposition of the reactant and the stability of the product.

CONCLUSIONS

(1) Electrolysis increases the decomposition rate of pseudoboehmite and lowers the onset temperature of the reaction at higher field strengths, especially at the negative electrode.

(2) The activation energy of the process is not significantly changed by electrolysis.

(3) The crystallite size of the product formed at the negative electrode is almost double that at the positive electrode.

(4) The electrolysis mechanism probably involves the weakening and cleavage of hydrogen bonds in the axis of the field, with the resulting protons migrating to the cathode by an interstitial mechanism. At the cathode, the protons are discharged as water or as hydrogen, or they may enter the structure of the decomposition product, enhancing its stability and crystallinity.

(5) The results support the suggestion that the formation of γ-alumina during low-temperature anodization of aluminium may be due to the electrolytic decomposition of a pseudoboehmite layer.

ACKNOWLEDGEMENTS

The author is indebted to Dr. R. S. Alwitt, United Chemi-Con Inc., for bringing the problem to his attention, and for supplying the pseudoboehmite sample. The scanning electron microscopy was carried out by Mr. G. D. Walker.

REFERENCES

1 B. C. Lippens and J. J. Steggerda, in B. G. Linsen (Ed.), *Physical and Chemical Aspects of Adsorbents and Catalysts*, Academic Press, New York, 1970, p. 171.
2 R. S. Alwitt, *J. Electrochem. Soc.*, 114 (1967) 843.
3 K. J. D. MacKenzie, *J. Therm. Anal.*, 5 (1973) 19.
4 R. S. Alwitt, *J. Colloid Interface Sci.*, 40 (1972) 195.
5 D. Papee, R. Tertian and R. Biais, *Bull. Soc. Chim. Fr.*, (1958) 1301.
6 V. Alevra, D. Ciomirtan and M. Ionescu, *Rev. Roum. Chim.*, 17 (1972) 1163.
7 K. J. D. MacKenzie and P. J. Melling, *Thermochim. Acta*, 9 (1974) 389.
8 I. F. Guilliatt and N. H. Brett, *J. Brit. Ceram. Soc.*, 6 (1969) 56.
9 J. H. Sharp, G. W. Brindley and B. N. Narahari Achar, *J. Am. Ceram. Soc.*, 49 (1966) 379.
10 C. Eyraud and R. Goton, *J. Chim. Phys.*, 51 (1954) 430.
11 W. D. Callister, I. B. Cutler and R. S. Gordon, *J. Am. Ceram. Soc.*, 49 (1966) 419.
12 J. Lima-de-Faria, *Z. Kristallogr.*, 119 (1963) 176.
13 V. Alevra, D. Ciomirtan and M. Ionescu, *Rev. Roum. Chim.*, 17 (1972) 1379.
14 G. M. M. Houben, *Refract. J.*, 28 (1952) 252.
15 J. J. Fripiat, H. Bosmans and P. G. Rouxhet, *J. Phys. Chem.*, 71 (1967) 1097.
16 A. Mata Arjona and J. J. Fripiat, *Trans. Faraday Soc.*, 63 (1967) 2936.
17 J. J. Fripiat and R. Touillaux, *Trans. Faraday Soc.*, 65 (1969) 1236.
18 H. F. W. Taylor, *Clay. Miner. Bull.*, 5 (1962) 45.
19 H. Saalfeld and B. B. Mehrotra, *Ber. Dtsch. Keram. Ges.*, 42 (1965) 161.
20 H. Frohlich, *Theory of Dielectrics*, Oxford, 1949, p. 12.
21 F. A. Cotton and G. Wilkinson, *Advanced Inorganic Chemistry*, Interscience, New York, 2nd ed., 1966, p. 213.

22 P. Gross and C. Hayman, *U.S. Gov. Res. Devel. Rept.*, 70 (1970) 71.
23 O. L. Kuskov, *Geokhimiya*, (1973) 348.
24 A. Navrotsky and O. J. Kleppa, *J. Inorg. Nucl. Chem.*, 30 (1968) 479.
25 A. Navrotsky and O. J. Kleppa. *J. Inorg. Nucl. Chem.*, 29 (1967) 2701.
26 K. J. D. MacKenzie, *J. Inorg. Nucl. Chem.*, 32 (1970) 3731.